bioRxiv preprint doi: https://doi.org/10.1101/2021.04.14.439775; this version posted April 14, 2021. The copyright holder for this preprint (which was not certified by peer review) is the author/funder, who has granted bioRxiv a license to display the preprint in perpetuity. It is made available under aCC-BY-NC-ND 4.0 International license.

1 **Phosphorus stress induces the synthesis of novel glycolipids in *Pseudomonas*
2 *aeruginosa* that confer protection against a last-resort antibiotic**
3
4 **Running title**: ecophysiology of lipid renovation in *Pseudomonas aeruginosa*
5
6 Rebekah A. Jones[1,2], Holly Shropshire[2], Caimeng Zhao[3], Andrew Murphy[2], Ian Lidbury[2,4],
7 Tao Wei[3], David J Scanlan[2], Yin Chen[2]
8
9
10 [1]MRC Doctoral Training Partnership, University of Warwick, Coventry, CV4 7AL, UK.
11
12 [2]School of Life Sciences, University of Warwick, Coventry, CV7, 7AL, UK
13
14 [3]School of Food and Biological Engineering, Zhengzhou University of Light Industry,
15 Zhengzhou, 450002, China
16
17 [4]Department of Animal and Plant Sciences, University of Sheffield, Sheffield, S10 1AE,
18 UK
19
20
21 Correspondence to Yin Chen, (email, y.chen.25@warwick.ac.uk, phone 00 44 24
22 76528976)
23
24 Classification: *Integrated genomics and post-genomics approaches in microbial ecology*

bioRxiv preprint doi: https://doi.org/10.1101/2021.04.14.439775; this version posted April 14, 2021. The copyright holder for this preprint (which was not certified by peer review) is the author/funder, who has granted bioRxiv a license to display the preprint in perpetuity. It is made available under aCC-BY-NC-ND 4.0 International license.

25 **Abstract**

26 *Pseudomonas aeruginosa* is a nosocomial pathogen with a prevalence in
27 immunocompromised individuals and is particularly abundant in the lung microbiome of
28 cystic fibrosis patients. A clinically important adaptation for bacterial pathogens during
29 infection is their ability to survive and proliferate under phosphorus limited growth
30 conditions. Here, we demonstrate that *P. aeruginosa* adapts to P-limitation by substituting
31 membrane glycerophospholipids with sugar-containing glycolipids through a lipid
32 renovation pathway involving a phospholipase and two glycosyltransferases. Combining
33 bacterial genetics and multi-omics (proteomics, lipidomics and metatranscriptomic
34 analyses), we show that the surrogate glycolipids monoglucosyldiacylglycerol and
35 glucuronic acid-diacylglycerol are synthesised through the action of a new phospholipase
36 (PA3219) and two glycosyltransferases (PA3218 and PA0842). Comparative genomic
37 analyses revealed that this pathway is strictly conserved in all *P. aeruginosa* strains
38 isolated from a range of clinical and environmental settings and actively expressed in the
39 metatranscriptome of cystic fibrosis patients. Importantly, this phospholipid-to-glycolipid
40 transition comes with significant ecophysiological consequence in terms of antibiotic
41 sensitivity. Mutants defective in glycolipid synthesis survive poorly when challenged with
42 polymyxin B, a last-resort antibiotic for treating multi-drug resistant *P. aeruginosa*. Thus,
43 we demonstrate an intriguing link between adaptation to environmental stress (nutrient
44 availability) and antibiotic resistance, mediated through membrane lipid renovation that is
45 an important new facet in our understanding of the ecophysiology of this bacterium in the
46 lung microbiome of cystic fibrosis patients.

bioRxiv preprint doi: https://doi.org/10.1101/2021.04.14.439775; this version posted April 14, 2021. The copyright holder for this preprint (which was not certified by peer review) is the author/funder, who has granted bioRxiv a license to display the preprint in perpetuity. It is made available under aCC-BY-NC-ND 4.0 International license.

47 **Introduction**

48 *P. aeruginosa* is a significant nosocomial pathogen in intensive care units causing
49 pneumonia, surgical wound site infections and sepsis (1-2). It is now recognised as a
50 leading cause of morbidity and mortality in chronically infected cystic fibrosis (CF) patients
51 and immunocompromised individuals due to the surge of carbapenem resistant strains, a
52 key group of first line antibiotics for treating *P. aeruginosa* infections (3). For these drug-
53 resistant *P. aeruginosa* strains, a viable but not ideal treatment option are polymyxins,
54 considered to be last resort antibiotics. Although polymyxins are active against *P.*
55 *aeruginosa*, their use was originally discontinued due to concerns over toxicity (4). Indeed,
56 *P. aeruginosa* has started to develop mechanisms of resistance to polymyxins due to an
57 increase in their use globally. These primarily include modifications to the
58 lipopolysaccharide (LPS) layer of the outer membrane through the addition of 4-amino-4-
59 deoxy-L-arabinose (L-Ara4N) or phosphoethanolamine (pEtN) (5-6). These changes
60 perturb the electrostatic interaction between cationic polymyxins and the normally
61 negatively charged LPS.
62
63 Glycerophospholipids, such as phosphatidylglycerol (PG) and phosphatidylethanolamine
64 (PE), are the major lipids forming the membrane lipid bilayer in bacteria, archaea and
65 eukaryotes (7-11). They play a fundamental role in the evolution of the cell and it is widely
66 accepted that the last universal common ancestor possessed a phospholipid membrane
67 (12-13). Although it is uncertain why evolution selected glycerophospholipids as the
68 building blocks for maintaining cellular membranes (13), it is known that organisms can
69 alter their membrane lipid composition in response to nutrient stress or environmental
70 changes (7, 14). Previous studies have firmly established the link between nutrient stress,
71 particularly phosphorus availability, and the expression of a variety of virulence factors in
72 *P. aeruginosa* (15-19). However, it is unclear whether adaptation to phosphorus limitation

bioRxiv preprint doi: https://doi.org/10.1101/2021.04.14.439775; this version posted April 14, 2021. The copyright holder for this preprint (which was not certified by peer review) is the author/funder, who has granted bioRxiv a license to display the preprint in perpetuity. It is made available under aCC-BY-NC-ND 4.0 International license.

73 in this bacterium causes a change in membrane lipid composition and, if so, whether lipid
74 remodelling comes with unforeseen ecophysiological consequences. Using a synthesis of
75 multi-omics approaches, here we show that *P. aeruginosa* produces surrogate glycolipids
76 to replace phospholipids in response to phosphorus limitation. These glycoglycerolipids
77 have not previously been reported in *P. aeruginosa*. This lipid renovation pathway is
78 strictly conserved in all *P. aeruginosa* strains isolated from a range of clinical settings and
79 actively expressed in the metatranscriptome of cystic fibrosis patients. Importantly, such
80 a phospholipid-to-glycolipid transition comes with a significant consequence in antibiotic
81 sensitivity, in that glycolipids confer protection when challenged with the antimicrobial
82 peptide polymyxin B. As such, glycolipid-mediated resistance to polymyxin B represents
83 a new resistance mechanism that is quite different from the previously documented
84 modification of LPS (5-6). This work highlights how the physiological adaptation of
85 *Pseudomonas aeruginosa* to phosphorus limitation can mediate a physiological response
86 that may have profound implications for the survival of the bacteria in the lung microbiome.
87
88

89 **Materials and methods**

90 **Cultivation of *P. aeruginosa* and mutants**

91 *P. aeruginosa* strain PAO1 was obtained from the DSMZ culture collection (Germany) and
92 routinely cultured in lysogeny broth (LB). A defined medium previously outlined for
93 *Pseudomonas* species to control phosphate levels was also used (20). This modified
94 minimal media A comprised: Na-succinate 20 mM, NaCl 200 mg L^{-1}, NH_4Cl 450 mg L^{-1},
95 $CaCl_2$ 200 mg L^{-1}, KCl 200 mg L^{-1}, $MgCl_2$ 450 mg L^{-1}, with trace metals $FeCl_2$ 10 mg L^{-1}
96 and $MnCl_2$ 10 mg L^{-1}, with 10 mM 4-(2-hydroxyethyl)-1-piperazineethanesulfonic acid
97 (HEPES) buffer used at pH 7. Na_2HPO_4 was then added to a final concentration of 50 μM
98 (low P) or 1 mM (high P). An intermediate phosphate source of 400 μM Na_2HPO_4 was

bioRxiv preprint doi: https://doi.org/10.1101/2021.04.14.439775; this version posted April 14, 2021. The copyright holder for this preprint (which was not certified by peer review) is the author/funder, who has granted bioRxiv a license to display the preprint in perpetuity. It is made available under aCC-BY-NC-ND 4.0 International license.

99 used for overnight cultures in some experiments to prevent any excess storage of
100 phosphate that could hamper results. All components were filter sterilised using 0.22 µm
101 pore-size filters, and made up using double deionised H_2O. Mutants were obtained from
102 the *P. aeruginosa* strain PAO1 transposon mutant library at the University of Washington,
103 and confirmed using PCR and subsequent sequencing.
104

105 **Alkaline phosphatase assay**

106 Alkaline phosphatase activity was monitored as a measure of Pi stress. Liquid *P.*
107 *aeruginosa* culture samples were incubated with 10 mM *para*-nitrophenol phosphate
108 (*p*NPP) to a final concentration of 1 mM. Yellow-*p*NP supernatant was measured in
109 triplicate at 407 nm (BioRad iMark microplate reader). Readings were normalised using
110 both a Tris-only incubation control and further by bacterial density (optical density reading
111 at 600 nm (OD_{600})).
112

113 **Over-expression of Agt1 and Agt2 in *E. coli***

114 *P. aeruginosa* genes PA3218 (*agt1*) and PA0842 (*agt2*) were codon optimised for *E. coli*
115 and chemically synthesised (GenScript) into plasmid pET-28a(+). *E. coli* BLR(DE3)
116 competent cells were thawed for 5 minutes before incubation with 10 ng pET-28a_Agt
117 plasmid, and placed on ice for 5 minutes. Cells were then subjected to heat shock at 42°C
118 for 30 seconds, placed back on ice for 2 minutes. Recovery SOC media was added, with
119 samples incubated at 37°C shaking, for 1 hour. Transformed cells were then plated onto
120 kanamycin-LB agar and grown overnight at 37°C. To harvest cells for lipid extraction,
121 single colonies were picked to grow in small volume LB-Kan to 0.6 OD_{600} before induction
122 with 0.4 mM IPTG overnight at 25°C. 1 mL samples were then pelleted at 10,000 x *g* for
123 5 minutes. Pellets were stored at -80°C until lipid extraction and subsequent analysis on
124 HPLC-MS.

bioRxiv preprint doi: https://doi.org/10.1101/2021.04.14.439775; this version posted April 14, 2021. The copyright holder for this preprint (which was not certified by peer review) is the author/funder, who has granted bioRxiv a license to display the preprint in perpetuity. It is made available under aCC-BY-NC-ND 4.0 International license.

125 To purify the Agt1 and Agt2 proteins from recombinant *E. coli*, IPTG was added to
126 a final concentration of 0.5 mM once the cultures reached an OD_{600} of 0.6. After a further
127 12 h of growth at 30°C, cells were harvested by centrifugation and resuspended in buffer
128 A containing 50 mM Tris-HCl, pH 7.9, 50 mM NaCl. Cells were disrupted by sonication
129 and 1% (w/v) triton X-100 was then added and the cells were then incubated for 2.5 hr at
130 4°C. The cells were then centrifuged at 12,000 × *g* for 20 min, and the soluble fraction
131 was loaded onto a nickel column (GE Healthcare, USA) pre-equilibrated with buffer A. The
132 recombinant Agt1 and Agt2 enzymes were eluted with an elution buffer (20 mM Tris-HCl,
133 pH 7.9, 500 mM NaCl, 300 mM imidazole) and dialyzed overnight into buffer A to remove
134 imidazole. For further purification, the samples were dialyzed overnight into buffer B
135 containing 50 mM Tris-HCl, pH 7.9, 200 mM NaCl, concentrated by ultrafiltration using a
136 30-kDa membrane (Millipore), and loaded onto a Superdex 200 (16/60) gel filtration
137 column (GE Healthcare, USA), which was pre-equilibrated with buffer B (50 mM Tris-HCl,
138 pH 7.9, 200 mM NaCl). The fraction size was 0.5 ml, and the flowrate was 0.5 ml/min.
139 Purified protein was analysed by SDS-PAGE, and protein concentrations were determined
140 using the Bradford assay.
141

142 **Membrane lipid extraction and HPLC-MS analysis**

143 Intact polar membrane lipids were extracted using a modified version of the typically used
144 Folch extraction method (21, 22). Liquid *P. aeruginosa* cultures growing in high and low
145 phosphate modified minimal medium A were sampled after 8 hrs, collecting the equivalent
146 of 0.5 OD_{600} into a 2 mL glass chromacol vial (Thermo Scientific), pelleted at 4°C, 4,000
147 rpm for 15 minutes. For lipid extraction, a ratio of 500:300:1000 μL of
148 methanol:water:chloroform (all LC-MS grade) was used. The lipid fraction was collected
149 from the lower phase using a glass Pasteur pipette. This chloroform extract was then dried
150 under a stream of nitrogen (Techne sample concentrator) and resuspended in 1 mL 95%

bioRxiv preprint doi: https://doi.org/10.1101/2021.04.14.439775; this version posted April 14, 2021. The copyright holder for this preprint (which was not certified by peer review) is the author/funder, who has granted bioRxiv a license to display the preprint in perpetuity. It is made available under aCC-BY-NC-ND 4.0 International license.

151 (v/v) acetonitrile (HPLC grade): 5% (w/v) ammonium acetate (10 mM, pH 9.2) for analysis.
152 Extracted lipid samples were analysed using an UltiMate 3000 HPLC (Thermo Scientific)
153 system coupled to an AmazonSL quadrupole ion trap (Bruker) mass spectrometer (MS),
154 using electrospray ionisation. Hydrophilic interaction chromatography (HILIC) using a
155 BEH amide XP column (Waters) was utilised to separate lipid classes based on their head
156 group (35). The column chamber was maintained at 30°C and the samples passed
157 through at a 150 µL min^{-1} flow rate. The mobile phase of acetonitrile:ammonium acetate
158 (pH 9.2) was used to elute the sample in a 15 minute per sample gradient, from 95% to
159 28% ammonium acetate. The lipid d17:1/12:0 sphingosylphosphoethanolamine (Sigma-
160 Aldrich, 50 nM) was added to the samples and used as an internal standard. Tandem MS
161 (or MS^n) was used to fragment the intact lipids for identification. The data were analysed
162 using the Bruker Compass software package (DataAnalysis and QuantAnalysis).
163
164 **Enzyme activity assays**
165 The glycosyltransferase activity of Agt1 and Agt2 was measured using uridine
166 diphosphate (UDP)-glucose or UDP-glucuronic acid and 0.1 mM C16:0/C18:1
167 diacylglycerol (DAG) as the substrate. 2.0 µM purified enzyme was used in 10 mM
168 Tricine/KOH buffer, pH 8.5 with 2 mM dithiothreitol. The resulting mixture (500 µl) was
169 incubated at 30°C for 60 min with constant shaking at 200 rpm. The lipid products were
170 extracted using the Folch method as described above. The lipid extracts were further
171 analysed by LC-MS for the identification of MGDG/GADG though MS^n fragmentation and
172 for the quantification of DAG against standards. The K_m and V_{max} values were calculated
173 using Michaelis-Menten plots with various concentrations of UDP-sugars (0.1 to 1.0 mM)
174 in three replicates.
175
176 **Antibiotic sensitivity assays**

bioRxiv preprint doi: https://doi.org/10.1101/2021.04.14.439775; this version posted April 14, 2021. The copyright holder for this preprint (which was not certified by peer review) is the author/funder, who has granted bioRxiv a license to display the preprint in perpetuity. It is made available under aCC-BY-NC-ND 4.0 International license.

177 *P. aeruginosa* cultures were grown to an OD_{600} of 0.6 in high or low phosphate minimal
178 media A (see above). Cultures were then diluted 1:100 in prewarmed minimal media A
179 containing 4 μg mL^{-1} polymyxin B sulfate (Sigma). Samples were incubated at 37°C, 180
180 rpm, and assayed for survivors at specified time points by serial dilution plating onto LB.
181 *E. coli* cultures containing pET-28a-Agt1 or pET-28a-Agt2 were grown to an OD_{600} of 0.6
182 in LB broth, and the expression of Agt1 and Agt2 was induced by incubation with 0.4 mM
183 IPTG overnight at 25°C. A negative control of *E. coli* containing the pET-28a vector only
184 was also set up. Overnight cultures were diluted 1:100 in prewarmed LB broth containing
185 0.4 mM IPTG and 20 μg mL^{-1} polymyxin B sulfate (Sigma). Samples were incubated at
186 37°C, 180 rpm, and assayed for survivors at specified time points by serial dilution plating
187 onto LB agar + kanamycin 25 μg mL^{-1}.
188
189 **Comparative proteomic analysis**
190 *P. aeruginosa* PAO1 WT (1 mM phosphate, 50 μM phosphate) and PlcP mutant (50 μM
191 phosphate) cell pellets in three biological replicates were resuspended in LDS (lithium
192 dodecyl sulfate) sample buffer containing 1% β-mercaptoethanol before lysing at 95°C
193 and vortexing. 30 μL of each sample were run on NuPAGE 10% Bis-Tris protein gel
194 (Invitrogen) for a short time before staining with SafeStain (Thermo Fisher) and excising
195 the whole protein band. In-gel proteins were de-stained using 50% (v/v) ethanol, 50 mM
196 ammonium bicarbonate (ABC), before being reduced and alkylated for 5 min at 70°C using
197 10 mM TCEP (tris(2-carboxyethyl)phosphine) and 40 mM CAA (2-chloroacetamide),
198 respectively. After washing with 50% (v/v) ethanol 50 mM ABC, peptides were lysed
199 overnight using trypsin. Finally, peptides were extracted by sonication in a water bath (10
200 min at room temperature), concentrated using a Speed-Vac (50 mins) and resuspended
201 in 2.5% acetonitrile 0.05% formic acid. Extracted peptides were analysed by nanoLC-ESI-
202 MS/MS using the Ultimate 3000/Orbitrap Fusion instrumentation (Thermo Scientific). The

bioRxiv preprint doi: https://doi.org/10.1101/2021.04.14.439775; this version posted April 14, 2021. The copyright holder for this preprint (which was not certified by peer review) is the author/funder, who has granted bioRxiv a license to display the preprint in perpetuity. It is made available under aCC-BY-NC-ND 4.0 International license.

203 UniProt proteome for *P. aeruginosa* strain PAO1 was used for peptide analysis. Further
204 data analysis was carried out using MaxQuant and Perseus software as described
205 previously; peptides without triplicate measures were filtered out (23). Comparative
206 proteomics data are presented in Supplementary Tables S1 and S3.
207

208 **Phylogenomics and metatranscriptomics analyses**

209 The protein sequences of PA3219, PA3218 and PA0842 were used to search genome
210 sequences of *Pseudomonas* clades in the JGI IMG genome portal
211 (https://img.jgi.doe.gov/). Note that the PA3218 protein is incorrectly annotated in the
212 genome of PAO1. The putative glycosyltransferase located immediately downstream of
213 PA3219 was manually inspected by aligning to the corresponding gene (PA14_22600) in
214 the genome of *P. aeruginosa* PA14. To identify PA3218 in misannotated *P. aeruginosa*
215 genomes, the nucleotide sequence immediately downstream of PA3219 was aligned with
216 *agt1* in strain PA14, (locus tag PA14_22600). The phylogeny of *Pseudomonas* clades was
217 determined using the nucleotide sequences of six housekeeping genes (*rpoB, rpoD,*
218 *dnaE, recA, atpD, gyrB*) retrieved from each genome using IQ-Tree with the parameters -
219 m TEST -bb 1000 -alrt 1000. The most suitable model was chosen by the software.
220 Evolutionary distances were inferred using maximum-likelihood analysis. Relationships
221 were visualised using the online platform the Interactive Tree of Life viewer
222 (https://itol.embl.de/). The conserved Pho box sequence was predicted using the MEME
223 server (24).

224 The metatranscriptomics datasets of sputum samples obtained from a CF patient
225 7-days (SRX5145606) and 8-days (SRX5145605) before death (25), CF patient G
226 (SRR6833349) from Denmark (26) and a patient (SRR6833340) with chronic wound
227 infection (26) were retrieved from the short reads archive (SRA) database
228 (https://www.ncbi.nlm.nih.gov/sra). The reads were downloaded using fastq-dump and

bioRxiv preprint doi: https://doi.org/10.1101/2021.04.14.439775; this version posted April 14, 2021. The copyright holder for this preprint (which was not certified by peer review) is the author/funder, who has granted bioRxiv a license to display the preprint in perpetuity. It is made available under aCC-BY-NC-ND 4.0 International license.

229 mapped using the BBMap aligner as described previously (27). Briefly, the SRA reads
230 were mapped to the genome sequence of *P. aeruginosa* PAO1 using a stringent cut-off
231 of minid=0.97. Relative abundance data were compared using RPKM (reads per kilobase
232 of transcript, per million mapped reads). The list of RPKM abundance of individual genes
233 of *P. aeruginosa* PAO1 is shown in **Suppl. Table S4**.
234
235
236 **Results and discussion**
237 ***P. aeruginosa* produces novel glycolipids in response to Pi stress**
238 To determine changes in the membrane lipidome in response to P-stress, the model *P.*
239 *aeruginosa* strain PAO1 was grown in minimal medium under high (1 mM) or low Pi (50
240 μM) conditions (**Figure 1a**). The latter condition elicited strong alkaline phosphatase
241 activity, measured through the liberation of *para*-nitrophenol (*p*NP) from *para*-nitrophenol
242 phosphate (*p*NPP) (**Figure 1b**), this being a strong indication that cells were P-stressed.
243 Analysis of membrane lipid profiles using high performance liquid chromatography
244 coupled to mass spectrometry (HPLC-MS) revealed the presence of several new lipids
245 under Pi stress conditions (**Figure 1c**). Thus, during Pi-replete growth (1 mM phosphate),
246 the lipidome is dominated by two glycerophospholipids: phosphatidylglycerol (PG, eluted
247 at 6.8 min) and phosphatidylethanolamine (PE, eluted at 12.2 min). During Pi-stress a lipid
248 species with mass to charge ratio (*m/z*) of 623 and 649 were also found, with MS
249 fragmentation resulting in a 131 *m/z* peak, a diagnostic ion for the amino-acid containing
250 ornithine lipid. This is consistent with previous reports of ornithine lipids in the *P.*
251 *aeruginosa* membrane in response to Pi stress (28-29).
252 Further to ornithine lipids, three unknown lipids eluting at 7.7 min, 8.7 min and 9.8
253 min, were only present under Pi stress conditions (**Figure 1c**). Using several rounds of
254 MS fragmentation (MS^n), with a quadrupole ion trap MS, fragmentation patterns

bioRxiv preprint doi: https://doi.org/10.1101/2021.04.14.439775; this version posted April 14, 2021. The copyright holder for this preprint (which was not certified by peer review) is the author/funder, who has granted bioRxiv a license to display the preprint in perpetuity. It is made available under aCC-BY-NC-ND 4.0 International license.

255 characteristic of glycolipids were found for all three peaks. For each peak of interest, the
256 most predominant lipid masses of 774.7 *m/z*, 786.8 *m/z* and 788.6 *m/z* were analysed by
257 MS^n in positive ionisation mode (**Figure 1d**). In each case, an initial head group was lost
258 leaving a significant signal of 595.6 *m/z*, the mass of the glycolipid building block
259 diacylglycerol (DAG). Further fragmentation leads to the loss of either fatty acyl chain from
260 DAG, leaving monoacylglycerols of 313.2 *m/z* and 339.3 *m/z*. Two monoacylglycerols with
261 different masses are produced as a result of the original lipid containing 16:0 and 18:1
262 fatty acids (313.2 *m/z* and 339.3 *m/z* monoacylglycerols, respectively). To further elucidate
263 the identity of the peaks, a search for a neutral loss of a polar head group was carried out.
264 Thus, the intact masses of 774.7 *m/z* and 788.6 *m/z* in positive ionisation mode leads to
265 the loss of a head group of -179 and -193 *m/z*, which corresponds to a hexose- and a
266 glucuronate- group, respectively (**Figure 1d**), suggesting the occurrence of novel
267 monoglucosyldiacylglycerol (MGDG) and glucuronic acid diacylglycerol (GADG)
268 glycolipids in *P. aeruginosa*. The third glycolipid peak at 8.7 min remains an unknown lipid
269 with intact mass of 786.8 *m/z* (hereafter designated as a putative unknown glycolipid,
270 UGL). Together, these data confirm the production of new glycolipids in *P. aeruginosa* in
271 response to Pi stress.
272

273 **Comparative proteomics uncover the lipid renovation pathway in *P. aeruginosa***

274 To determine the proteomic response of *P. aeruginosa* to phosphorus limitation, and
275 identify the genes involved in glycolipid formation, strain PAO1 was cultivated under high
276 and low Pi conditions for 8 hours and the cellular proteome then analysed. A total of 2844
277 proteins were detected, 175 of which were found to be differentially regulated by Pi
278 availability (**Figure 2b, Suppl. Table S1**). In line with previous transcriptomic studies of
279 strain PAO1 (18), major phosphorus acquisition mechanisms were highly expressed

bioRxiv preprint doi: https://doi.org/10.1101/2021.04.14.439775; this version posted April 14, 2021. The copyright holder for this preprint (which was not certified by peer review) is the author/funder, who has granted bioRxiv a license to display the preprint in perpetuity. It is made available under aCC-BY-NC-ND 4.0 International license.

280 under Pi stress conditions, *e.g.* the Pi-specific transporter PstSCAB, the two-component
281 regulator PhoBR (**Suppl. Table S1**) (30).

282 Comparative proteomics also identified several genes which are likely important
283 for membrane lipid remodelling (**Figure 2a**) including PA3219 (4.6-fold increase under Pi-
284 depleted conditions, FDR<0.01), encoding a putative phospholipase C protein, and
285 PA0842 (4-fold increase under Pi-depleted conditions, FDR<0.01), encoding a putative
286 glycosyltransferase (**Figure 2b**). PA3219 has 47% protein sequence identity to PlcP from
287 *Phaeobacter* sp. MED193 and 46% identity to PlcP from *Sinorhizobium meliloti* (25-27).
288 In these bacteria, PlcP is essential in the lipid remodelling pathway for the formation of the
289 diacylglycerol (DAG) backbone, representing the essential intermediate for the production
290 of glycolipids (31-32). In *P. aeruginosa* PAO1, PA3219 appears to form an operon with
291 PA3218, a putative glycosyltransferase likely under the control of the PhoBR two
292 component system, as a highly conserved Pho box sequence was recognisable in the
293 promoter region (**Figure 2c**). PA3218 (hereafter referred to as Agt1) has 41% protein
294 sequence identity to the Agt of *Phaeobacter* sp. MED193. PA0842 showed 35% identity
295 to the Agt of *Phaeobacter* sp. MED193 and a Pho box sequence is also found in its
296 promoter region. This corroborates the finding that the PA0842 protein (hereafter referred
297 to as Agt2) was significantly upregulated under Pi-depleted conditions (**Figure 2b**). In
298 summary, comparative proteomic analysis suggests that *P. aeruginosa* PAO1 adopts this
299 PlcP-Agt lipid remodelling pathway for the production of glycolipids in response to Pi-
300 stress (**Figure 2a**).

301

302 **The PlcP-Agt mediated lipid renovation pathway is strictly conserved in *P.***
303 ***aeruginosa* and actively transcribed in the metatranscriptomes of cystic fibrosis**
304 **patients**

bioRxiv preprint doi: https://doi.org/10.1101/2021.04.14.439775; this version posted April 14, 2021. The copyright holder for this preprint (which was not certified by peer review) is the author/funder, who has granted bioRxiv a license to display the preprint in perpetuity. It is made available under aCC-BY-NC-ND 4.0 International license.

305 To uncover how widespread this predicted PlcP-Agt lipid remodelling pathway is amongst
306 the genus *Pseudomonas,* including *P. aeruginosa* strains, we conducted a thorough
307 comparative genomics analysis of these lipid renovating loci. PlcP-Agt is strictly conserved
308 in all 770 genome-sequenced *P. aeruginosa* strains in the IMG/M database, including all
309 three-previously recognised *P. aeruginosa* lineages (33-34), group 1 represented by strain
310 PAO1, group 2 represented by strain PA14 and group 3 represented by strain PA7 (**Figure**
311 **3, Suppl. Table S2**). Indeed, this remodelling pathway is prevalent in many *Pseudomonas*
312 groups, including the plant pathogen *Pseudomonas syringae*. To investigate whether the
313 PlcP-Agt lipid remodelling pathway is involved in host-pathogen interactions, we analysed
314 metatranscriptomic datasets from cystic fibrosis patients, where *P. aeruginosa* is known
315 to be prevalent in the fatal exacerbation period before patient death (25). To the best of
316 our knowledge, only two studies have reported the metatranscriptome of the bacterial
317 community present in CF sputum (25, 26). Indeed, *phoBR* and *pstS* are amongst the most
318 highly expressed genes, confirming previous observations that *P. aeruginosa* is Pi-limited
319 during human airway epithelia infection (36, 37). Interestingly, the alkaline phosphatase
320 *phoA* (38) was highly expressed in sputum from CF patients but not from wound samples
321 which was also dominated by *P. aeruginosa*. Importantly, the transcripts of *P. aeruginosa*
322 *agt1/plcP/agt2* are highly expressed in CF sputum during the fatal exacerbation period
323 before death (**Figure 2d**). Therefore, our phylogenomic and metatranscriptomic analyses
324 suggest that not only is the PlcP-Agt lipid remodelling pathway strictly conserved and
325 prevalent in *P. aeruginosa*, but also the corresponding genes are also highly expressed
326 during CF patient infection, suggesting a potential role for lipid renovation in host-
327 pathogen interactions.
328

329 **Experimental validation of the lipid renovation pathway for glycolipid formation in**
330 ***P. aeruginosa***

bioRxiv preprint doi: https://doi.org/10.1101/2021.04.14.439775; this version posted April 14, 2021. The copyright holder for this preprint (which was not certified by peer review) is the author/funder, who has granted bioRxiv a license to display the preprint in perpetuity. It is made available under aCC-BY-NC-ND 4.0 International license.

331 To validate the function of these two putative glycosyltransferases (Agt1, Agt2) in the
332 formation of glycolipids, we synthesized the codon-optimized genes (PA3218 and
333 PA0842, respectively) for recombinant expression in *Escherichia coli*. The total lipidomes
334 from the recombinant *E. coli* strains were then analysed by HPLC-MS to determine the
335 presence of glycolipids in a gain-of-function assay. Expression of *P. aeruginosa* Agt1
336 (PA3218) was sufficient for the production of MGDG (eluted at 7.7 min) in *E. coli*,
337 confirmed through MS^n fragmentation (**Figure 4a**). No UGL nor GADG was observed in
338 the lipidome of this Agt1-overexpressing *E. coli* strain. Expressing Agt2 (PA0842) from *P.*
339 *aeruginosa* in *E. coli* was sufficient for the accumulation of the GADG glycolipid (eluted at
340 9.8 min), also confirmed through the MS^n fragmentation pattern (**Figure 4b**). Equally, no
341 UGL nor MGDG was observed in the Agt2-overexpressing *E. coli* strain. Production of
342 these glycolipids was not observed in the same strain of *E. coli* transformed with an empty
343 vector control (pET28a). It is therefore likely that UGL production is carried out by another
344 glycosyltransferase, the identity of which remains to be discovered.

345 To confirm the role of Agt1 and Agt2 in the production of MGDG and GADG, we
346 purified Agt1 and Agt2 from recombinant *E. coli* (**Figure 4c**) and carried out enzyme
347 assays using UDP-glucose and UDP-glucuronic acid as the sugar donor and DAG as the
348 acceptor. Agt1 can only accept UDP-glucose as the substrate with an affinity of K_m=298.1
349 ± 9.5 μM (**Figure 4c**, middle panel) and produced MGDG as expected (**Figure 4d**, left
350 panel). Similarly, Agt2 can use UDP-glucuronic acid as the substrate (K_m= 373.0 ± 12.9
351 μM (**Figure 4c**, right panel), producing the GADG lipid (**Figure 4d**, right panel).
352 Interestingly, the purified Agt2 enzyme can also use UDP-glucose to some extent with a
353 K_m of 480 μM (data not shown) although the corresponding lipid MGDG was not observed
354 in the lipid extract from the lipidome of the recombinant host *E. coli* (**Figure 4b**).

355 To further confirm the role of these genes in *P. aeruginosa* glycolipid biosynthesis
356 we analysed the lipidomes of mutants in *ΔplcP*, *Δagt1* and *Δagt2* in strain PAO1 (**Figure**

bioRxiv preprint doi: https://doi.org/10.1101/2021.04.14.439775; this version posted April 14, 2021. The copyright holder for this preprint (which was not certified by peer review) is the author/funder, who has granted bioRxiv a license to display the preprint in perpetuity. It is made available under aCC-BY-NC-ND 4.0 International license.

357 **5a, b**). Differences were analysed by searching for the intact masses of the glycolipids
358 MGDG and GADG: 774.6 *m/z* and 788.6 *m/z* in positive ionisation mode with an
359 ammonium adduct, respectively. As expected, under Pi stress MGDG is no longer
360 produced in the *Δagt1* mutant and similarly GADG is no longer produced in the *Δagt2*
361 mutant (**Figure 5a**). In the *ΔplcP* mutant, no MGDG was found and the GADG lipid was
362 significantly reduced but not entirely abolished (**Figure 5b**). The small amount of GADG
363 produced in the *ΔplcP* mutant suggests that an alternative supply of DAG (independent of
364 the degradation of phospholipids by PlcP) is available in this mutant. Nevertheless,
365 lipidome analyses of the *ΔplcP*, *Δagt1* and *Δagt2* mutants strongly supports the key role
366 of this PlcP-Agt pathway (**Figure 2A**) in lipid renovation in *P. aeruginosa*.
367

368 **The protective role of glycolipids to antibiotic resistance in *Pseudomonas***
369 ***aeruginosa***

370 To assess whether the growth of the glycolipid-deficient mutants (*ΔplcP*, *Δagt1*, *Δagt2*)
371 was affected by Pi stress, we grew the mutants in the defined minimal medium under high
372 and low Pi conditions. However, no significant difference in growth rates was found (Suppl.
373 Figure S1). The presence of glycolipids in the membrane may, however, have a profound
374 impact on the functioning of the membrane during Pi stress. For example, PG is an anionic
375 lipid with net negative charges whereas MGDG has a neutral charged sugar group.
376 Although a PG-to-GADG substitution may not necessarily change membrane charge (35),
377 it may affect membrane curvature and the packing density of lipids. Thus, subsequent
378 knock-on effects in membrane function might be expected (10). We therefore set out to
379 investigate whether membrane lipid composition may have an impact on antibiotic
380 resistance in *P. aeruginosa*. As cationic antimicrobial peptides directly interact with
381 bacterial cell membranes, we focused on the impact of lipid remodelling on the killing
382 activity of polymyxin B. We conducted the analyses under P-depleted conditions, since

bioRxiv preprint doi: https://doi.org/10.1101/2021.04.14.439775; this version posted April 14, 2021. The copyright holder for this preprint (which was not certified by peer review) is the author/funder, who has granted bioRxiv a license to display the preprint in perpetuity. It is made available under aCC-BY-NC-ND 4.0 International license.

383 Pi-stress is clinically important, already known to induce the expression of virulence
384 factors (15, 17, 18, 29), and our own analysis confirmed that an array of genes involved
385 in phosphate acquisition and lipid remodelling in *P. aeruginosa* are indeed highly
386 expressed in sputum samples from lung microbiome of CF patients (**Figure 2d**).
387 Polymyxins represent the drug-of-last resort for effectively treating carbapenem-resistant
388 *P. aeruginosa* infections (3, 39).

389 To test the sensitivity of the mutants in the PlcP-Agt pathway to polymyxin B, we
390 compared WT and mutants using kill curve analyses as the typically used disk diffusion
391 method does not work efficiently for cationic antimicrobials (40). Indeed, there was a
392 significant decrease in the survival of all three PAO1 glycolipid synthesis mutants (*ΔplcP*,
393 *Δagt1* and *Δagt2*) compared to the wild type when challenged with polymyxin B,
394 suggesting a protective role of glycolipids in polymyxin B resistance (**Figure 5c**). Such a
395 protective role of glycolipids in polymyxin B resistance was not observed for other
396 antibiotics, including ciprofloxacin, gentamicin, ceftazidime and meropenem (data not
397 shown). *P. aeruginosa* is known to enhance its resistance to polymyxins through
398 decoration of its lipopolysaccharide (LPS) layer using either 4-amino-4-deoxy-L-arabinose
399 (L-Ara4N) by *arnB* (5), or the addition of phosphoethanolamine (pEtN) by *eptA* (6). It is
400 thought that these changes perturb the electrostatic interaction between the cationic
401 polymyxin B and the normally negatively charged LPS. To investigate whether these
402 mechanisms play a role in the glycolipid-deficient mutants, we conducted a comparative
403 proteomics analysis of the *ΔplcP* mutant and WT under Pi depleted conditions, which
404 revealed only a small number of differentially expressed proteins (**Suppl. Table S3**). The
405 majority of these differentially expressed proteins are uncharacterised. However,
406 importantly, LPS modification enzymes previously found to confer antimicrobial peptide
407 resistance, such as ArnB and EptA, were not differentially expressed between the WT and
408 *ΔplcP* mutant. Therefore, our data suggests that it is the glycolipids that are the major

bioRxiv preprint doi: https://doi.org/10.1101/2021.04.14.439775; this version posted April 14, 2021. The copyright holder for this preprint (which was not certified by peer review) is the author/funder, who has granted bioRxiv a license to display the preprint in perpetuity. It is made available under aCC-BY-NC-ND 4.0 International license.

409 contributor to increased polymyxin B resistance, which constitutes a new biological
410 mechanism for polymyxin resistance. To this end, we tested the resistance to polymyxin
411 B of recombinant *E. coli* strains overexpressing *P. aeruginosa* Agt1 and Agt2, that produce
412 MGDG and GADG, respectively (**Figure 4a, 4b**). Indeed, in this gain-of-function assay,
413 both Agt1 and Agt2 overexpressing *E. coli* strains had enhanced resistance to polymyxin
414 B compared to the empty vector control (**Figure 5d**), supporting the protective role of
415 these glycolipids to antimicrobial peptides.
416
417 To conclude, we present here the discovery of novel glycolipids produced in *P.*
418 *aeruginosa* during adaption to phosphorus stress. This lipid renovation pathway is strictly
419 conserved in all *P. aeruginosa* isolates to date and highly expressed in the
420 metatranscriptome of CF patients, suggesting a key role of lipid remodelling in the
421 ecophysiology of this bacterium. Interestingly, lipid remodelling as a response to survive
422 phosphorus stress in turn comes with trade-offs in terms of antibiotic resistance; these
423 glycolipids may protect the bacterium from insult by cationic antimicrobial peptides,
424 highlighting a new resistance mechanism to polymyxin B which has been previously
425 overlooked. It remains to be seen whether the altered susceptibility to polymyxin B is the
426 sole trade-off following lipid remodelling of phospholipids to glycolipids. After all, evolution
427 appears to have selected phospholipids as the dominant lipids in the last universal
428 common ancestor (12).
429
430 **Acknowledgements**

431 This work was funded by an MRC Doctoral Training Partnership studentship in
432 Interdisciplinary Biomedical Research (MR/J003964/1) awarded to RAJ and by a Royal
433 Society International Exchanges 2017 Cost Share (China) award (IEC\NSFC\170213; grant
434 agreement no. 170213). AM and YC are supported by a European Research Council (ERC)

bioRxiv preprint doi: https://doi.org/10.1101/2021.04.14.439775; this version posted April 14, 2021. The copyright holder for this preprint (which was not certified by peer review) is the author/funder, who has granted bioRxiv a license to display the preprint in perpetuity. It is made available under aCC-BY-NC-ND 4.0 International license.

435 award under the European Union's Horizon 2020 research and innovation programme
436 (grant agreement no. 726116). We also thank the Proteomics Research Technology
437 Platform, University of Warwick, UK for their contribution.

438

439 **Competing interest**

440 The authors declare no competing interests.

bioRxiv preprint doi: https://doi.org/10.1101/2021.04.14.439775; this version posted April 14, 2021. The copyright holder for this preprint (which was not certified by peer review) is the author/funder, who has granted bioRxiv a license to display the preprint in perpetuity. It is made available under aCC-BY-NC-ND 4.0 International license.

441 **References**

442 **1.** Murray, T. S., Egan, M., & Kazmierczak, B. I. (2007). *Pseudomonas aeruginosa*
443 chronic colonization in cystic fibrosis patients. *Curr. Opin. Pediatr.,* 19: 83-88.
444 **2.** Gaynes, R., Edwards, J. R., & System, N. N. I. S. (2005). Overview of nosocomial
445 infections caused by Gram-negative bacilli. *Clin. Infect. Dis.*, 41:848–854.
446 **3.** Hawkey PM, Livermore DM (2012). Carbapenem antibiotics for serious infections.
447 *BMJ*. 344:e3236.
448 **4.** Landman, D., Georgescu, C., Martin, D. A., & Quale, J. (2008). Polymyxins
449 revisited. *Clin. Microbiol. Rev*. 21:449–465.
450 **5.** Chung, E. S., Lee, J. Y., Rhee, J. Y., & Ko, K. S. (2017). Colistin resistance in
451 *Pseudomonas aeruginosa* that is not linked to *arnB*. *J. Med. Microbiol.*, 66:833–
452 841.
453 **6.** Nowicki, E. M., O'Brien, J. P., Brodbelt, J. S., & Trent, M. S. (2015). Extracellular
454 zinc induces phosphoethanolamine addition to *Pseudomonas aeruginosa* lipid A
455 via the ColRS two-component system. *Mol. Microbiol. 97*:166–178.
456 **7.** Parsons JB, Rock CO. (2013) Bacterial lipids: metabolism and membrane
457 homeostasis. *Prog. Lipid Res.* 52:249-276.
458 **8.** Zhang, Y.-M., & Rock, C. O. (2008). Membrane lipid homeostasis in bacteria. *Nat.*
459 *Rev. Microbiol.* 6:222–233.
460 **9.** van Meer G, Voelker DR, Feigenson GW. (2008) Membrane lipids: where they are
461 and how they behave. *Nat. Rev. Mol. Cell Biol.* 9:112-124.
462 **10.** Harayama T, Riezman H. (2018) Understanding the diversity of membrane lipid
463 composition. *Nat. Rev. Mol. Cell Biol.* 19:281-296.
464 **11.** May, K.L., & Silhavy T.J. (2017) Making a membrane on the other side of the wall.
465 *Biochim. et Biophy. Acta*. 1862:1386-1393.
466 **12.** Lombard J, López-García P, Moreira D. (2012) The early evolution of lipid
467 membranes and the three domains of life. *Nat. Rev. Microbiol.* 10:507-515.
468 **13.** Peretó J, López-García P, Moreira D. (2004) Ancestral lipid biosynthesis and early
469 membrane evolution. *Trends Biochem. Sci*. 29:469-477.
470 **14.** Sahonero-Canavesi DX, López-Lara IM, Geiger O (2019) Membrane lipid
471 degradation and lipid cycles in microbes. In *Aerobic Utilization of Hydrocarbons,*
472 *Oils, and Lipids*, 10.1007/978-3-319-50418-6_38
473 **15.** Lamarche MG, Wanner BL, Crépin S, Harel J. (2008) The phosphate regulon and
474 bacterial virulence: a regulatory network connecting phosphate homeostasis and
475 pathogenesis. *FEMS Microbiol. Rev.* 32:461-473.

bioRxiv preprint doi: https://doi.org/10.1101/2021.04.14.439775; this version posted April 14, 2021. The copyright holder for this preprint (which was not certified by peer review) is the author/funder, who has granted bioRxiv a license to display the preprint in perpetuity. It is made available under aCC-BY-NC-ND 4.0 International license.

476 **16.** Long, J., Zaborina, O., Holbrook, C., Zaborin, A., & Alverdy, J. (2008). Depletion of
477 intestinal phosphate after operative injury activates the virulence of *P. aeruginosa*
478 causing lethal gut-derived sepsis. *Surgery*, *144*:189–197.
479 **17.** Francis VI, Stevenson EC, Porter SL. (2017) Two-component systems required for
480 virulence in *Pseudomonas aeruginosa. FEMS Microbiol. Lett.* 364(11). doi:
481 10.1093/femsle/fnx104.
482 **18.** Bains, M., Fernández, L., & Hancock, R. E. W. (2012). Phosphate starvation
483 promotes swarming motility and cytotoxicity of *Pseudomonas aeruginosa*. *Appl.*
484 *Environ. Microbiol.*, *78*:6762–6768.
485 **19.** Son, M. S., Matthews, W. J., Kang, Y., Nguyen, D. T., & Hoang, T. T. (2007). *In*
486 *vivo* evidence of *Pseudomonas aeruginosa* nutrient acquisition and pathogenesis
487 in the lungs of cystic fibrosis patients. *Infect. Immun.* 75:5313–5324.
488 **20.** Lidbury, I. D. E. A., Murphy, A. R. J., Scanlan, D. J., Bending, G. D., Jones, A. M.
489 E., Moore, J. D., et al., (2016). Comparative genomic, proteomic and exoproteomic
490 analyses of three *Pseudomonas* strains reveals novel insights into the phosphorus
491 scavenging capabilities of soil bacteria. *Environ. Microbiol.* 18:3535–3549.
492 **21.** Sebastián, M., Smith, A. F., González, J. M., Fredricks, H. F., Van Mooy, B.,
493 Koblížek, M., et al., (2016). Lipid remodelling is a widespread strategy in marine
494 heterotrophic bacteria upon phosphorus deficiency. *ISME J.* 10:968–978.
495 **22.** Smith AF, Rihtman B, Stirrup R, Silvano E, Mausz MA, Scanlan DJ, Chen Y. (2019)
496 Elucidation of glutamine lipid biosynthesis in marine bacteria reveals its importance
497 under phosphorus deplete growth in *Rhodobacteraceae. ISME J.* 13:39-49.
498 **23.** Shropshire H, Jones RA, Aguilo-Ferretjans MM, Scanlan DJ, Chen Y. (2021)
499 Proteomics insights into the *Burkholderia cenocepacia* phosphorus stress
500 response. doi.org/10.1111/1462-2920.15451.
501 **24.** Bailey TL, Elkan C (1994) Fitting a mixture model by expectation maximization to
502 discover motifs in biopolymers. *Proceedings of the Second International*
503 *Conference on Intelligent Systems for Molecular Biology*, 28-36, AAAI Press,
504 Menlo Park, Californias.
505 **25.** Cobián Güemes AG, Lim YW, Quinn RA, Conrad DJ, Benler S, Maughan H,
506 Edwards R, et al. (2019) Cystic fibrosis rapid response: translating multi-omics data
507 into clinically relevant information. *mBio.* 16;10(2):e00431-19.
508 **26.** Cornforth DM, Dees JL, Ibberson CB, Huse HK, Mathiesen IH, Kirketerp-Moller K,
509 et al., (2018) *Pseudomonas aeruginosa* trascriptome during human infection. *Proc.*
510 *Nat. Acad. Sci. USA* 115:E5125-5134.

bioRxiv preprint doi: https://doi.org/10.1101/2021.04.14.439775; this version posted April 14, 2021. The copyright holder for this preprint (which was not certified by peer review) is the author/funder, who has granted bioRxiv a license to display the preprint in perpetuity. It is made available under aCC-BY-NC-ND 4.0 International license.

511 **27.** Jones, H.J., Krober, E., Stephenson, J., Mausz M.A., Jameson, E., Millard, A.,
512 Purdy, K.J., Chen, Y. (2019) A new family of uncultivated bacteria involved in
513 methanogenesis from the ubiquitous osmolyte glycine betaine in coastal saltmarsh
514 sediments. *Microbiome*. 7, 120. doi.org/10.1186/s40168-019-0732-4
515 **28.** Kim, S. K., Park, S. J., Li, X. H., Choi, Y. S., Im, D. S., & Lee, J. H. (2018). Bacterial
516 ornithine lipid, a surrogate membrane lipid under phosphate-limiting conditions,
517 plays important roles in bacterial persistence and interaction with host. *Environ.*
518 *Microbiol. 20*:3992–4008.
519 **29.** Lewenza, S., Falsafi, R., Bains, M., Rohs, P., Stupak, J., Sprott, G. D., & Hancock,
520 R. E. W. (2011). The *olsA* gene mediates the synthesis of an ornithine lipid in
521 *Pseudomonas aeruginosa* during growth under phosphate-limiting conditions, but
522 is not involved in antimicrobial peptide susceptibility. *FEMS Microbiol. Lett.* 320:
523 95–102.
524 **30.** Wilton M, Halverson TW, Charron-Mazenod L, Parkins MD, Lewnza S. (2018)
525 Secreted phosphatase and deoxyribonuclease are required by *Pseudomonas*
526 *aeruginosa* to defend against neutrophil extracellular traps. *Infect. Immun*
527 86:e00403-18.
528 **31.** Wei, T., Quareshy, M., Zhang, Y. Z., Scanlan, D. J., & Chen, Y. (2018). Manganese
529 is essential for PlcP metallophosphoesterase activity involved in lipid remodeling
530 in abundant marine heterotrophic bacteria. *Appl. Environ. Microbiol. 84,* e01109-
531 18.
532 **32.** Zavaleta-Pastor, M., Sohlenkamp, C., Gao, J.-L., Guan, Z., Zaheer, R., Finan, T.
533 M., et al., (2010). *Sinorhizobium meliloti* phospholipase C required for lipid
534 remodeling during phosphorus limitation. *Proc. Nat. Acad. Sci. USA107*:302–307.
535 **33.** Freschi L, Jeukens J, Kukavica-Ibrulj I, Boyle B, Dupont MJ, Laroche J, et al.,
536 (2015) Clinical utilization of genomics data produced by the international
537 *Pseudomonas aeruginosa* consortium. *Front Microbiol.* 29;6:1036. doi:
538 10.3389/fmicb.2015.01036.
539 **34.** Ozer EA, Nnah E, Didelot X, Whitaker RJ, Hauser AR. (2019) The population
540 structure of *Pseudomonas aeruginosa* is characterized by genetic isolation of
541 *exoU*+ and *exoS*+ lineages. *Genome Bio.l Evol.* 11:1780-1796.
542 **35.** Diercks H, Semeniuk A, Gisch N, Moll H, Duda KA, Hölzl G. (2015) Accumulation
543 of novel glycolipids and ornithine lipids in *Mesorhizobium loti* under phosphate
544 deprivation. *J. Bacteriol.* 197:497-509.
545 **36.** Chugani, SA and Greenberg, EP (2007) The influence of human respiratory

bioRxiv preprint doi: https://doi.org/10.1101/2021.04.14.439775; this version posted April 14, 2021. The copyright holder for this preprint (which was not certified by peer review) is the author/funder, who has granted bioRxiv a license to display the preprint in perpetuity. It is made available under aCC-BY-NC-ND 4.0 International license.

546 epithelia on *Pseudomonas aeruginosa* gene expression. *Microb. Pathog.* 42: 29–
547 35.
548 **37.** Frisk, A, Schurr, JR, Wang, G, Bertucci, DC, Marrero, L, Hwang, SH, et al. (2004)
549 Transcriptome analysis of *Pseudomonas aeruginosa* after interaction with human
550 airway epithelial cells. *Infect. Immun.* 72: 5433–5438.
551 **38.** Filloux A, Bally M, Soscia C, Murgier M, Lazdunski A (1988) Phsphate regulation
552 in *Pseudomonas aeruginosa*: Clonning of the alkaline phosphatase gene and
553 identification of *phoB* and *phoR*-like gnes. *Mol. Gen. Genet* . 212(3):510-513.
554 **39.** Poirel L, Jayol A, Nordmann P. (2017) Polymyxins: antibacterial activity,
555 susceptibility testing, and resistance mechanisms encoded by plasmids or
556 chromosomes. *Clin. Microbiol. Rev*. 30:557-596.
557 **40.** Ezadi, F., Ardebili A., Mirnead R (2019) Antimicrobial susceptibility testing for
558 polymyxins: challenges, issues, and recommendations. *J. Clin. Microbiol. 57,*
559 e01390-18.
560 **41.** Monds RD, Newell PD, Schwartzman JA, O'Toole GA. (2006) Conservation of the
561 Pho regulon in *Pseudomonas fluorescens* Pf0-1. *Appl. Environ. Microbiol*.
562 72:1910-1924.
563 **42.** Semeniuk A, Sohlenkamp C, Duda K, Hölzl G. (2014) A bifunctional
564 glycosyltransferase from *Agrobacterium tumefaciens* synthesizes monoglucosyl
565 and glucuronosyl diacylglycerol under phosphate deprivation. *J. Biol. Chem.*
566 289(14):10104-10114.
567 **43.** Minh BQ, Schmidt HA, Chernomor O, Schrempf D, Woodhams MD, von
568 Haeseler A, et al. (2020) IQ-TREE 2: New models and efficient methods for
569 phylogenetic inference in the genomic era. *Mol. Biol. Evol*. 37:1530–1534.
570

bioRxiv preprint doi: https://doi.org/10.1101/2021.04.14.439775; this version posted April 14, 2021. The copyright holder for this preprint (which was not certified by peer review) is the author/funder, who has granted bioRxiv a license to display the preprint in perpetuity. It is made available under aCC-BY-NC-ND 4.0 International license.

571 **Figure legends**

572 **Figure 1 Lipidomics analysis uncovers novel glycolipid formation in *Pseudomonas***
573 ***aeruginosa* strain PAO1 in response to phosphorus limitation.**

574 **a)** Growth of strain PAO1 WT in minimal medium A containing 1 mM phosphate (+Pi, blue)
575 or 50 μM phosphate (-Pi, black) over 12 hours. Data are the average of 3 independent
576 replicates.

577 **b)** Liberation of *para*-nitrophenol (*p*NP) from *para*-nitrophenol phosphate (*p*NPP) through
578 alkaline phosphatase activity, under Pi-repleted (1 mM, black) and Pi-depleted (50 μM,
579 yellow) conditions. Error bars represent the standard deviation of three independent
580 replicates.

581 **c)** Representative chromatograms in negative ionisation mode of the *P*. *aeruginosa*
582 lipidome when grown under phosphorus stress (-Pi, black) compared to growth under
583 phosphorus sufficient conditions (+Pi, orange). PG, phosphatidylglycerol; PE,
584 phosphatidylethanolamine, OL, ornithine lipids. Lower panel: extracted ion
585 chromatograms of three new glycolipid species in *P. aeruginosa* which are only produced
586 during Pi-limitation (black, 1 mM; orange, 50 μM). MGDG: monoglucosyldiacylglycerol,
587 GADG: glucuronic acid-diacylglycerol and UGL: unconfirmed glycolipid.

588 **d)** Mass spectrometry fragmentation spectra of three glycolipid species present under Pi
589 stress in *P. aeruginosa*, at retention times of 7.7 (*m/z* 774.7), 8.7 (*m/z* 786.7) and 9.8 (*m/z*
590 788.6) minutes, respectively. Each spectrum depicts an intact lipid mass with an
591 ammonium (NH_4^+) adduct exhibiting neutral loss of a head group, yielding diacylglycerol
592 (DAG) (595 *m/z*). Further fragmentation yields monoacylglycerols (MAG) with C16:0 or
593 C18:1 fatty acyl chains.

594

bioRxiv preprint doi: https://doi.org/10.1101/2021.04.14.439775; this version posted April 14, 2021. The copyright holder for this preprint (which was not certified by peer review) is the author/funder, who has granted bioRxiv a license to display the preprint in perpetuity. It is made available under aCC-BY-NC-ND 4.0 International license.

595 **Figure 2 Comparative multi-omic analyses for the identification of the PlcP-Agt**
596 **pathway responsible for glycolipid formation in *Pseudomonas aeruginosa* strain**
597 **PAO1.**

598 **a)** The proposed pathway for lipid remodelling through the PlcP-Agt pathway. PlcP
599 degrades membrane phospholipids such as PG, to generate diacylglycerol (DAG)
600 intermediates for the formation of MGDG and GADG through the activity of
601 glycosyltransferases, using either UDP-glucose or UDP-glucuronate as the co-substrate
602 (42).

603 **b)** Volcano plot depicting differentially expressed proteins when comparing Pi-repleted
604 and Pi-depleted conditions. Significantly upregulated proteins when under Pi stress are
605 shown in red (left), and those that are significantly upregulated when Pi is sufficient are in
606 green (right). Significance was accepted when the false discovery rate (FDR) was < 0.05,
607 and a fold change ≥ 2.

608 **c)** Genomic organisation of predicted lipid remodelling genes in *P. aeruginosa*.
609 Glycosyltransferases (orange) PA3218 (Agt1) and PA0842 (Agt2) are predicted to be
610 involved in glycolipid synthesis. PA3219 is predicted to be PlcP in *P. aeruginosa*.
611 Predicted Pho box sequences in the promoter regions (represented in blue boxes) of each
612 glycosyltransferase operon from *P. aeruginosa* strains representing the PAO1 clade, the
613 PA7 clade and the PA14 clade are shown. The black dots represent residues which are
614 conserved in the Pho box consensus CTGTCATNNNNCTGTCAT (41).

615 **d)** Metatranscriptomic analysis of PlcP-Agt lipid remodelling genes in sputum samples
616 from a cystic fibrosis patient 7-days (CF_D-7) and 8-days (CF_D-8) before death (25) and
617 a Danish CF patient (CF_Person G) (26) as well as a wound sample from a burns patient
618 from the USA (Burn patient) (26). Relative abundance is expressed as RPKM (reads per

bioRxiv preprint doi: https://doi.org/10.1101/2021.04.14.439775; this version posted April 14, 2021. The copyright holder for this preprint (which was not certified by peer review) is the author/funder, who has granted bioRxiv a license to display the preprint in perpetuity. It is made available under aCC-BY-NC-ND 4.0 International license.

619 kilobase of transcript, per million mapped reads). PhoA (PA3296) encodes an alkaline
620 phosphatase (38).

621
622 **Figure 3 Occurrence of *plcP-agt* genes in major *Pseudomonas* groups.** The
623 phylogeny of *Pseudomonas* clades was determined using the nucleotide sequences of six
624 housekeeping genes (*rpoB, rpoD, dnaE, recA, atpD, gyrB*) retrieved from each genome
625 using IQ-Tree (43). The filled colour indicates the presence of the genes in the genomes
626 whereas a blank indicates the absence of the corresponding gene in the genomes. The
627 two-component system PhoBR (black circles) is found in all genomes and the PlcP-
628 Agt1/Agt2 are strictly conserved in all 770 genome-sequenced *P. aeruginosa* strains that
629 form three clades represented by strain PA14, PA01 and PA7 respectively. Bootstrap
630 values >75% are shown.

631

632 **Figure 4**, **Characterization of glycolipid formation from recombinant Agt1 and Agt2.**
633 **a)** Extracted ion chromatogram of the MGDG lipid from recombinant *E. coli* expressing
634 Agt1. An empty vector control is also shown (red line). The identity of MGDG is further
635 validated using mass spectrometry fragmentation showing the neutral loss of 179
636 corresponding to the loss of glucose and the formation of monoacylglycerols (MAG) with
637 C16:0 or C18:1 (*m/z* 313.2, 339.3).

638 **b)** Extracted ion chromatogram of the GADG lipid from recombinant *E. coli* expressing
639 Agt2. An empty vector control is also shown (red line). The identity of GADG is further
640 validated using mass spectrometry fragmentation showing the neutral loss of 193
641 corresponding to the loss of glucose and the formation of monoacylglycerols (MAG) with
642 C16:0 or C18:1 (*m/z* 313.2, 339.2).

bioRxiv preprint doi: https://doi.org/10.1101/2021.04.14.439775; this version posted April 14, 2021. The copyright holder for this preprint (which was not certified by peer review) is the author/funder, who has granted bioRxiv a license to display the preprint in perpetuity. It is made available under aCC-BY-NC-ND 4.0 International license.

643 **c)** Purified Agt1 and Agt2 protein from recombinant *E. coli* (left panel) and Michaelis
644 Menten kinetics of Agt1 towards UDP-glucose (middle panel) and Agt2 towards UDP-
645 glucuronic acid (right panel) as substrate, respectively.

646 **d)** Mass spectrometry identification of MGDG and GADG produced from purified Agt1 and
647 Agt2 using DAG and UDP-glucose and UDP-glucuronic acid as the substrate,
648 respectively.

649

650 **Figure 5 Glycolipid formation in *P. aeruginosa* and mutants under Pi stress,**
651 **showing a protective role of glycolipids to polymyxin B.**

652 **a-b)** Relative abundance of the glycolipid MGDG (**a**) and GADG (**b**) in *P. aeruginosa*
653 mutants *plcP* (purple trace), *agt1* (blue trace) and *agt2* (green, trace) compared to the wild
654 type (WT). Cells were cultivated under low Pi conditions (50 μM) and a representative
655 extracted ion chromatogram of MGDG/GADG is shown between the WT, (black trace) and
656 each mutant. The right most panel shows the abundance of MGDG or GADG calculated
657 relative to an internal lipid standard d17:1/12:0 sphingosylphosphoethanolamine (Sigma-
658 Aldrich) in the wild-type and mutant strains of *P. aeruginosa*. Values are calculated from
659 three biological replicates and the error bars denote standard deviation. MGDG,
660 monoglucosyldiacylglycerol, GADG, glucuronic acid-diacylglycerol.

661 **c)** Survival of glycolipid remodelling mutants Δ*plcP* (purple), Δ*agt1* (green) and Δ*agt2*
662 (blue) when challenged with 4 μg mL^{-1} polymyxin B compared to WT under Pi stress
663 (black). All experiments were conducted under Pi stress conditions and the results are the
664 average of three biological replicates; error bars denote standard deviation.

665 **d)** Survival of glycolipid producing *Escherichia coli* when challenged with 20 μg mL^{-1}
666 polymyxin B. All experiments were conducted in three replicates and error bars denote

bioRxiv preprint doi: https://doi.org/10.1101/2021.04.14.439775; this version posted April 14, 2021. The copyright holder for this preprint (which was not certified by peer review) is the author/funder, who has granted bioRxiv a license to display the preprint in perpetuity. It is made available under aCC-BY-NC-ND 4.0 International license.

667 standard deviation. Black, *E. coli* containing the empty vector pET28a; green, *E. coli*
668 containing plasmid pET28a-Agt1; blue, *E. coli* containing plasmid pET28a-Agt2.
669

bioRxiv preprint doi: https://doi.org/10.1101/2021.04.14.439775; this version posted April 14, 2021. The copyright holder for this preprint (which was not certified by peer review) is the author/funder, who has granted bioRxiv a license to display the preprint in perpetuity. It is made available under aCC-BY-NC-ND 4.0 International license.

670 **Supplementary Figures and Tables**

671

672 **Suppl. Figure S1** Growth of the *P. aeruginosa* mutants in the minimal medium under Pi
673 repleted and Pi depleted conditions.

674

675 **Suppl. Table S1** Proteomic analysis of differentially expressed proteins in the wild-type
676 *P. aeruginosa* PAO1 in response to different Pi levels (1 mM versus 50 μM).

677

678 **Suppl. Table S2** Protein BLAST identification of locus tags homologous to *agt1* and *agt2*
679 glycolipid synthesis genes in all genome sequenced *P. aeruginosa* strains at the JGI IMG
680 database.

681

682 **Suppl. Table S3** Proteomic analysis of wild type *P. aeruginosa* PAO1 versus the Δ*plcP*
683 mutant grown at 50 μM Pi.

684

685 **Suppl. Table S4** Whole genome mapping to *Pseudomonas aeruginosa* PAO1 of
686 metatranscriptomic datasets (SRX5145605, SRX5145606, SRR6833349) from sputum
687 samples taken from cystic fibrosis patients and a patient with chronic wound infection
688 (SRR6833340). **S4A** (SRX5145605)**,** **S4B** (SRX5145606), **S4C** (SRR6833349), **S4D**
689 (SRR6833340)**.** RPKM, reads per kilobase of transcript per million mapped reads; FPKM,
690 fragments per kilobase of transcript per million mapped reads.

bioRxiv preprint doi: https://doi.org/10.1101/2021.04.14.439775; this version posted April 14, 2021. The copyright holder for this preprint (which was not certified by peer review) is the author/funder, who has granted bioRxiv a license to display the preprint in perpetuity. It is made available under aCC-BY-NC-ND 4.0 International license.

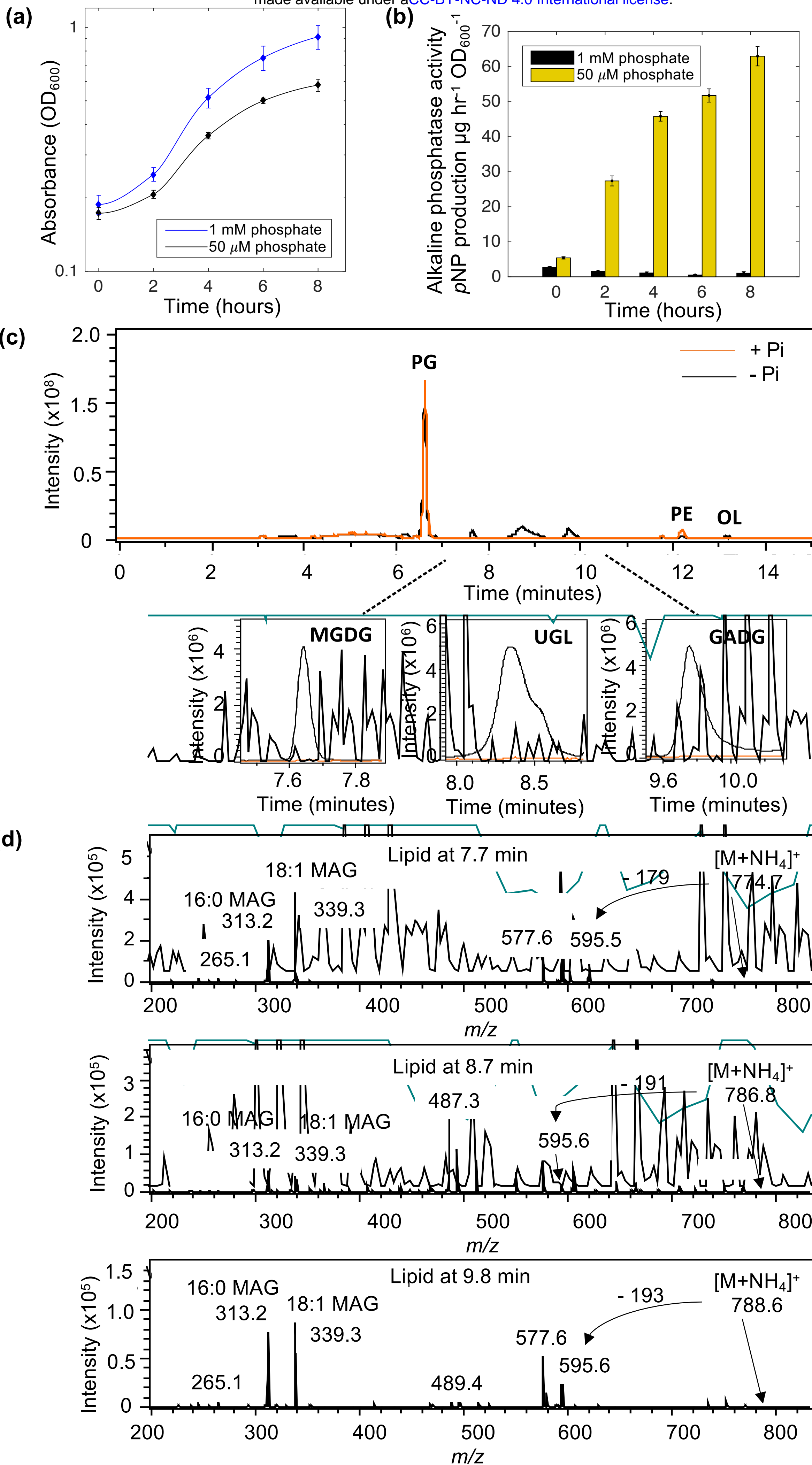

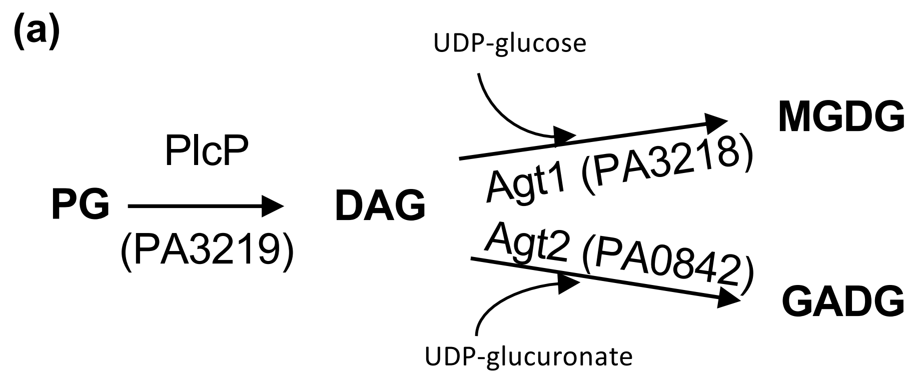
(a)
UDP-glucose
PlcP
PG
(PA3219)
DAG
Agt1 (PA3218)
MGDG
Agt2 (PA0842)
GADG
UDP-glucuronate
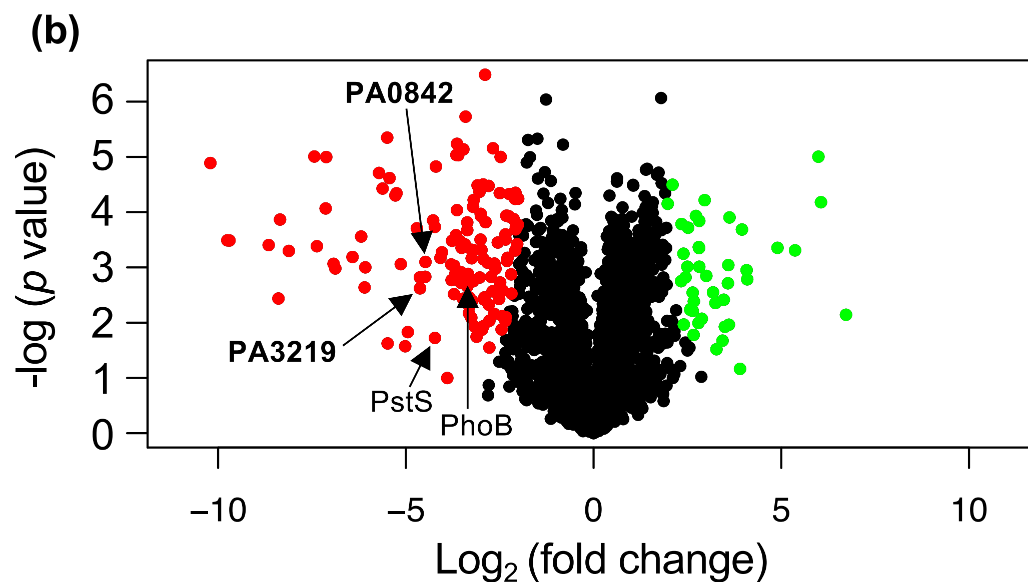
(b)
PA0842
PA3219
PstS
PhoB
-log (p value)
Log2 (fold change)
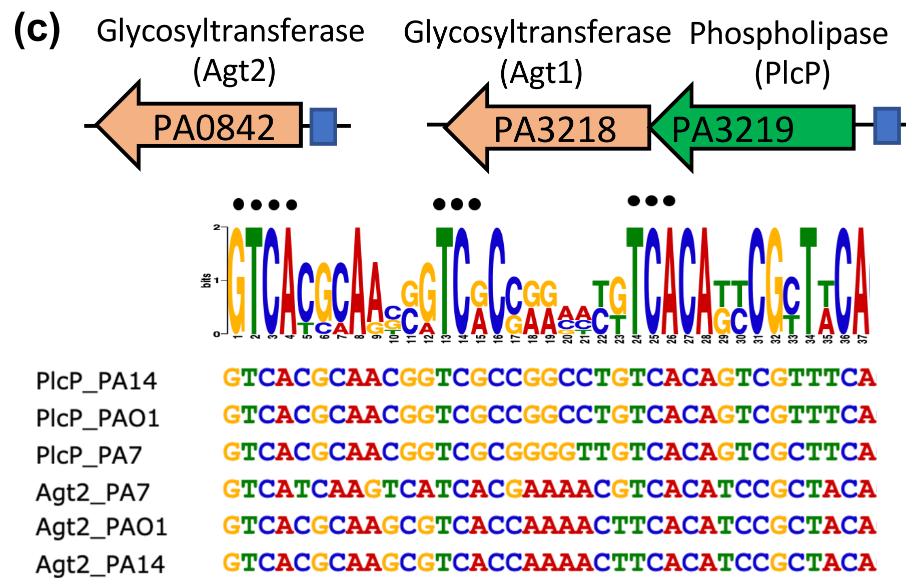
(c)
Glycosyltransferase (Agt2)
Glycosyltransferase (Agt1)
Phospholipase (PlcP)
PA0842
PA3218
PA3219
PlcP_PA14 GTCACGCAACGGTCGCCGGCCTGTCACAGTCGTTTCA
PlcP_PAO1 GTCACGCAACGGTCGCCGGCCTGTCACAGTCGTTTCA
PlcP_PA7 GTCACGCAACGGTCGCGGGGTTGTCACAGTCGCTTCA
Agt2_PA7 GTCATCAAGTCATCACGAAAACGTCACATCCGCTACA
Agt2_PAO1 GTCACGCAAGCGTCACCAAAACTTCACATCCGCTACA
Agt2_PA14 GTCACGCAAGCGTCACCAAAACTTCACATCCGCTACA
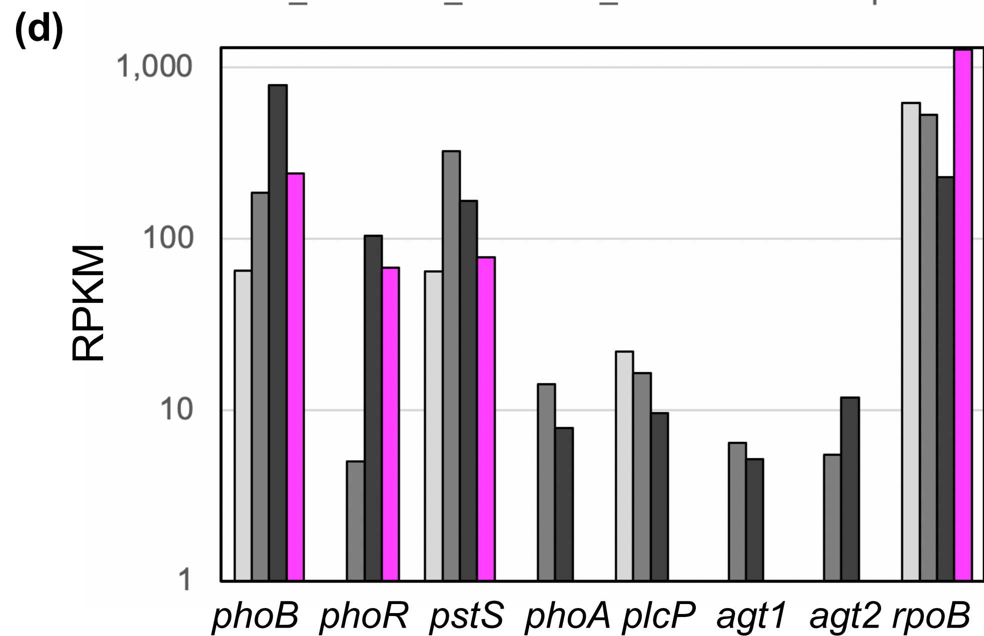
(d)
CF_D-7 CF_D-8 CF_Person G Burn patient
RPKM
phoB phoR pstS phoA plcP agt1 agt2 rpoB

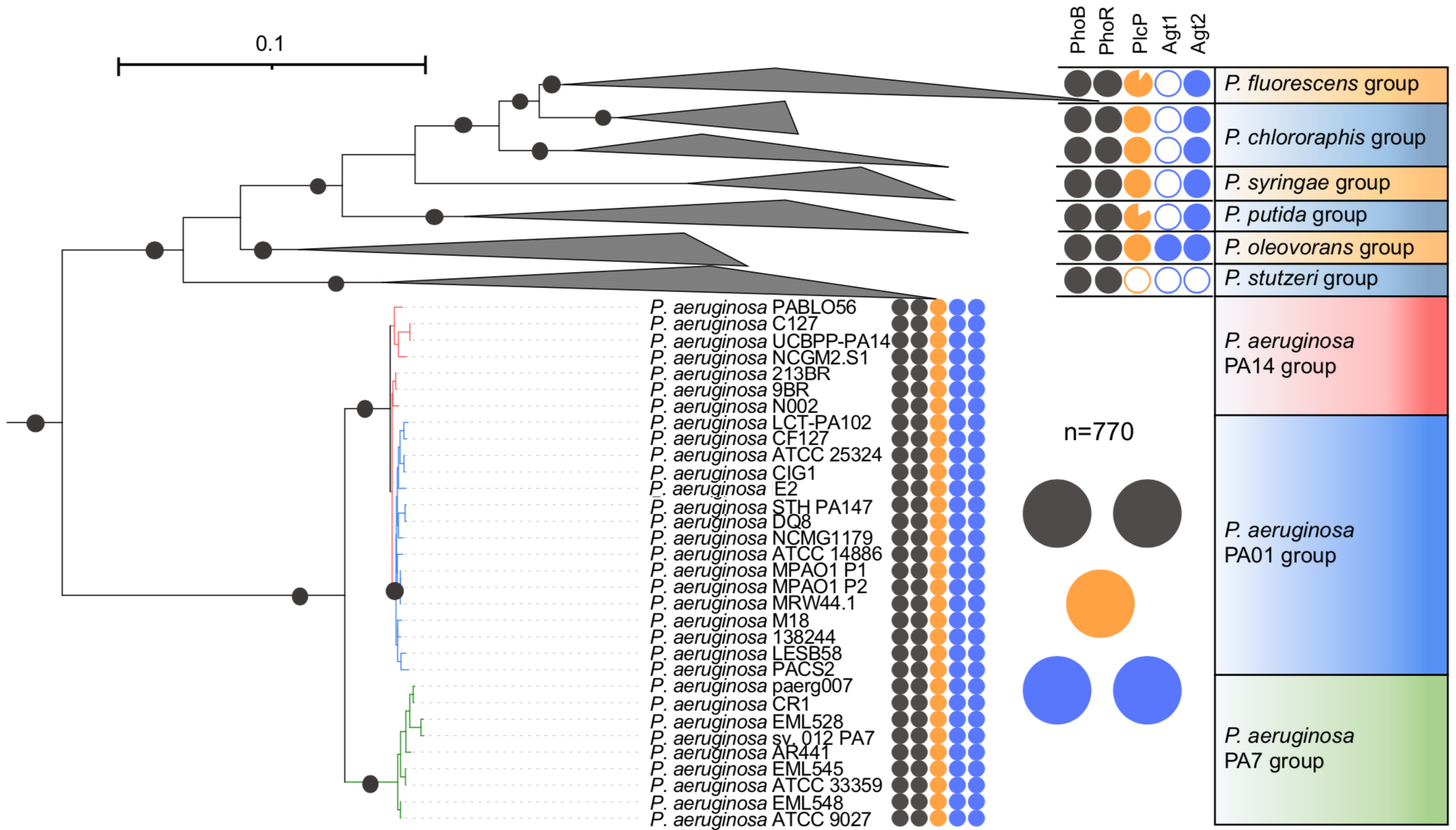
0.1
PhoB
PhoR
PlcP
Agt1
Agt2
P. fluorescens group
P. chlororaphis group
P. syringae group
P. putida group
P. oleovorans group
P. stutzeri group
P. aeruginosa PA14 group
P. aeruginosa PA01 group
P. aeruginosa PA7 group
n=770
P. aeruginosa PABLO56
P. aeruginosa C127
P. aeruginosa UCBPP-PA14
P. aeruginosa NCGM2.S1
P. aeruginosa 213BR
P. aeruginosa 9BR
P. aeruginosa N002
P. aeruginosa LCT-PA102
P. aeruginosa CF127
P. aeruginosa ATCC 25324
P. aeruginosa CIG1
P. aeruginosa E2
P. aeruginosa STH PA147
P. aeruginosa DQ8
P. aeruginosa NCMG1179
P. aeruginosa ATCC 14886
P. aeruginosa MPAO1 P1
P. aeruginosa MPAO1 P2
P. aeruginosa MRW44.1
P. aeruginosa M18
P. aeruginosa 138244
P. aeruginosa LESB58
P. aeruginosa PACS2
P. aeruginosa paerg007
P. aeruginosa CR1
P. aeruginosa EML528
P. aeruginosa sv. 012 PA7
P. aeruginosa AR441
P. aeruginosa EML545
P. aeruginosa ATCC 33359
P. aeruginosa EML548
P. aeruginosa ATCC 9027

bioRxiv preprint doi: https://doi.org/10.1101/2021.04.14.439775; this version posted April 14, 2021. The copyright holder for this preprint (which was not certified by peer review) is the author/funder, who has granted bioRxiv a license to display the preprint in perpetuity. It is made available under aCC-BY-NC-ND 4.0 International license.

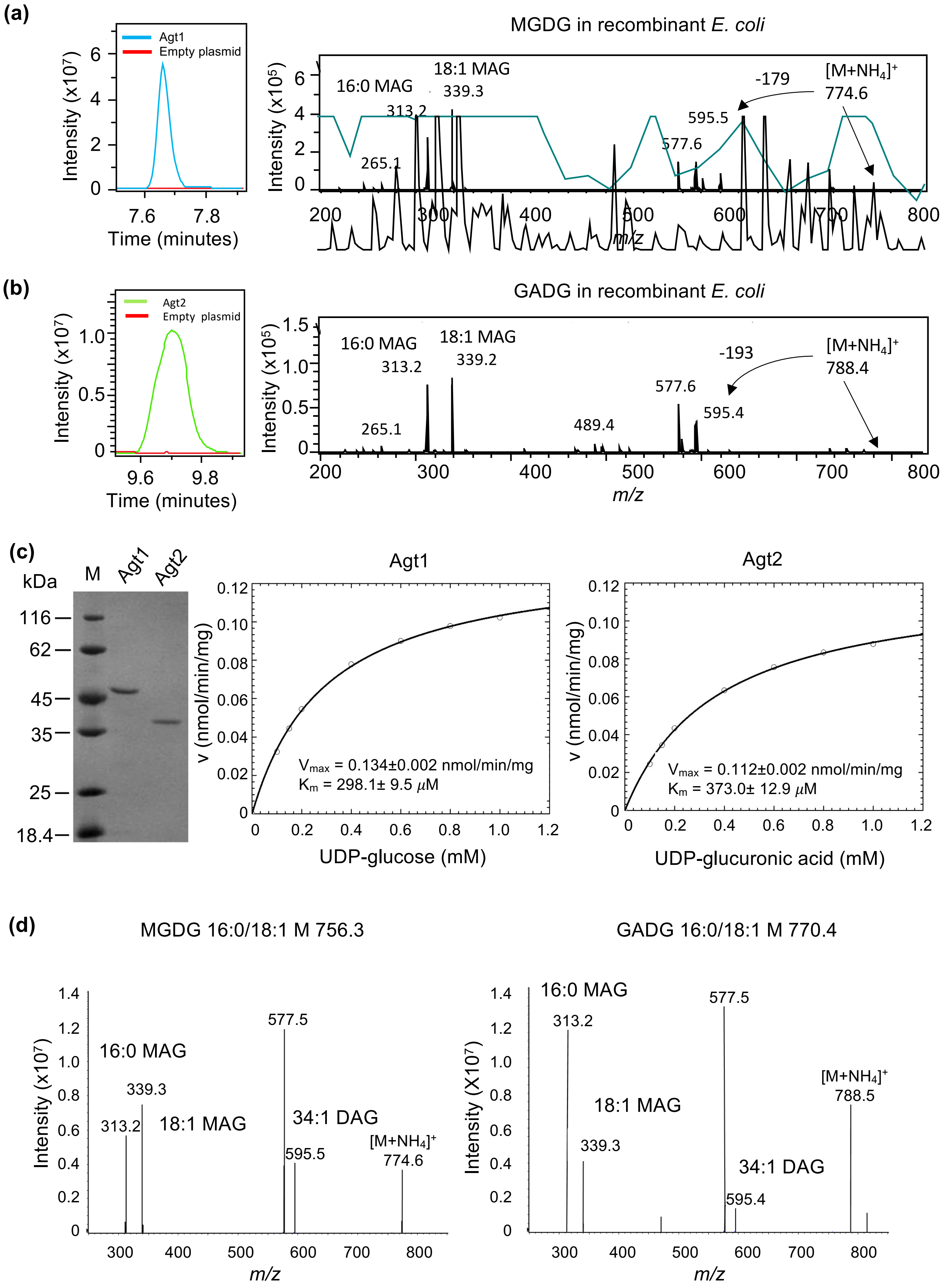

bioRxiv preprint doi: https://doi.org/10.1101/2021.04.14.439775; this version posted April 14, 2021. The copyright holder for this preprint (which was not certified by peer review) is the author/funder, who has granted bioRxiv a license to display the preprint in perpetuity. It is made available under aCC-BY-NC-ND 4.0 International license.